

H. M. SIDKI, M. AMER, F. ABD EL AZIZ

National Institute of Standards  
Laboratory of Engineering and Precise Optics  
Tersa Street, El-Haram, Giza, Code No. 12211, Egypt.  
email: hossamsidki@yahoo.com.

## CALIBRATION OF REFERENCE STANDARD QUARTZ ROTATING PLATES

An accurate linear polarized optical system for calibrating the quartz plate angles is introduced in this work. The quartz plate parallelism and surface roughness are measured using a phase shifting laser interferometer to study their effects on quartz rotation angles which equals to  $\pm 18.21$  sec. A polynomial regression method is applied to determine and extrapolate quartz rotation angles corresponds to the un-calibrated regions of the visible spectrum. The bi-rotation index values ( $n_L - n_R$ ) of the quartz plates for all scanned wavelengths are determined applying the calibrated rotation angles. The uncertainty of the calibrations is evaluated, also the combined uncertainty of calibrations for angles ( $\Delta\beta_i \approx \pm 0.09^\circ$ ) that shows the usefulness of this article.

Keywords: quartz rotating plates, phase shifting laser interferometer, polarization optical system

### 1. INTRODUCTION

Quality control of pharmaceutical, chemical and food industries depends on measuring the degree of concentration of optically active materials such as organic compounds using polarimeters. They are accurately calibrated by reference standard quartz rotating plates. The quartz rotating plates are also required to be calibrated to realize their traceability which is a difficult process due to their high accuracy.

Crystal quartz is a very useful material because of its high UV (ultra-violet), VIS (visible spectrum) and NIR (near infra red) transmittance, birefringence, ability to rotate plane polarized light, high damage threshold and resistance to scratching. Quartz is a crystalline form of silicon dioxide ( $\text{SiO}_2$ ). It is a hard, brittle, transparent material with a density of  $2649 \text{ kg/m}^3$  and a melting point of  $1750^\circ\text{C}$ . Quartz rotating crystals belong to the crystallographic class 32, and they are hexagonal prisms with six cap faces at each end, as shown in Fig. 1. In the case of a quartz uni-axial crystal cut perpendicular to its optic axis, the state of polarization for a beam after passing through the crystal remains unchanged. In the left quartz the E-field of an incident linear plane wave rotates anti-clockwise when seen by an observer looking towards the source of light, and in the right quartz it rotates clockwise. The d-rotatory and l-rotatory behavior in quartz is produced from two different crystallographic structures. Although the molecules are identical, crystal quartz can be either right- or left-handed depending on the arrangement of those molecules as shown in Fig. 1.

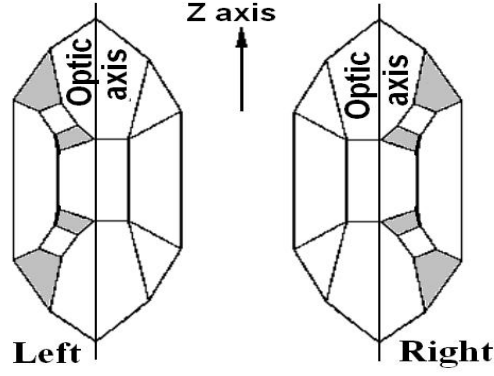


Fig. 1. Left- and right-handed quartz crystals are hexagonal prisms with six cap faces of crystallographic class 32.

The external appearances of these two forms are the same in all respects except that one is the mirror image of the other. [1, 2].

When a beam of plane-polarized light is transmitted along the optic axis, a rotation of the E-field of an incident linear plane wave occurs, and the amount of the rotation depends on the distance traversed in the material. Optical activity occurs when left-circular and right-circular polarizations have different propagation velocities. A linearly polarized wave will decompose into left- and right circular waves and become more and more out of phase as they propagate through the birefringent crystal. When the wave is re-expressed as linear polarization at some distance away, the E-field of an incident linear plane wave has rotated. A logical description of optical activity is explained as the superposition of *R*- and *L*- circular states waves that propagate at different speeds (Fig. 2).

An optically active material exhibits circular birefringence, i.e. it has two different rotation indices that cause the rotation of plane e. m. waves, one for *R*-states ( $n_R$ ) and one for *L*-states ( $n_L$ ). In traversing an optically active specimen the two circular waves would get out of phase and the resultant linear wave would appear to have rotated. When two monochromatic right- and left- circular light waves propagate in the *Z*-direction, they can be given by:

$$E_R = \frac{E_0}{2} [i \cos(k_R - \omega t) + j \sin(k_R - \omega t)], \quad (1) \quad [1]$$

$$E_L = \frac{E_0}{2} [i \cos(k_L - \omega t) + j \sin(k_L - \omega t)], \quad (2) \quad [1]$$

where:  $\omega$  is constant,  $k_R = k_0 n_R$  and  $k_L = k_0 n_L$ .

The resultant disturbance is given by  $E = E_R + E_L$  after mathematical treatment, it becomes

$$E = E_0 \cos \left[ \frac{z}{2} (k_R + k_L) - \omega t \right] \left[ i \cos(k_R - k_L) \frac{z}{2} + j \sin(k_R - k_L) \frac{z}{2} \right]. \quad (3)$$

At the position where the wave enters the medium ( $z = 0$ ) it is a linear plane wave along the *x*-axis as shown in Fig. 2, therefore it can be given by:

$$E = E_0 i \cos \omega t. \quad (4)$$

The two right- and left-circular waves have the same time dependence and are in phase.

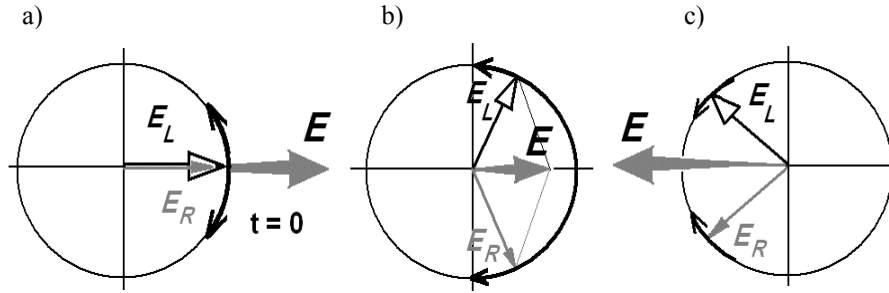


Fig. 2. The superposition of an  $R$ - and an  $L$ -state at  $Z=0$ .

The  $E$  field at any point  $z$  makes an angle of  $\beta = -(k_R - k_L) z/2$  with respect to its original orientation. If the medium has a thickness  $d$ , the rotation of the plane of vibration is then [1, 3]

$$\beta = \pi d (n_L - n_R) / \lambda, \quad (5)$$

where:  $\pi = 180$  degrees,  $(n_R)$  and  $(n_L)$  are the rotation indices or right and left directions for a plane e.m. wave. The difference  $(n_L - n_R)$  therefore can be called as the bi-rotation indices.

## 2. METHOD

Two reference standard quartz plates produced by Bellingham & Stanly Ltd. of England are studied in this article. The first is type 34-20 and the second is type 34-10. Quartz rotation angles are calibrated using an optical system working by linear polarized light since the rotation of linearly plane waves can be distinguished and accurately calibrated. The calibration of quartz plates requires to study surface parameters such as parallelism and surface roughness of the quartz plate surfaces in order to evaluate their effects on the accuracy of the plate's rotation angles. These parameters are studied by applying a phase shifting laser interferometer.

### 2.1. Interferometerical study of quartz's surface.

Since thickness of the quartz plate is the path length that causes rotation of the linear plane wave, thus the effect of non-parallelism of quartz plate's surfaces which cause thickness variation must be studied. Also, the effects of flatness and roughness of the quartz surfaces on the rotation angles are studied using a Zygo GPI-X phase shifting laser interferometer which is illustrated in Fig. 3.

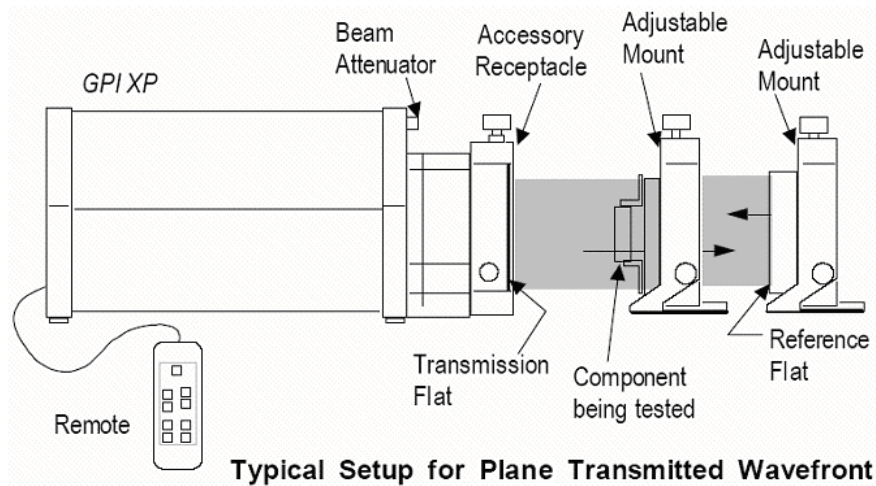


Fig. 3. A diagram of the phase shifting laser interferometer Zygo GPI-XP.

The Zygo GPI-XP is a Fizeau laser interferometer used to test the quartz rotating plate by comparing it against the reference flat. The instrument is useful for measuring the wedge angle of nearly parallel plates of diameter up to 95 mm.

The instrument has a built-in He-Ne laser ( $\lambda = 632.8 \text{ nm}$ ) as a source of light, a CCD camera for recording the interference fringes and a computer-based data acquisition system to measure the fringe spacing and analyze the data to convert them to the a large test aperture of 102 mm. Figure 4 shows the optical design of the Zygo GPI-Xp interferometer procured by Zygo Corporation (USA). The interferometer provides high quality, non-contact measurement of a wide variety of surface types. The measurements include non-parallelism, flatness and roughness of objects [4].

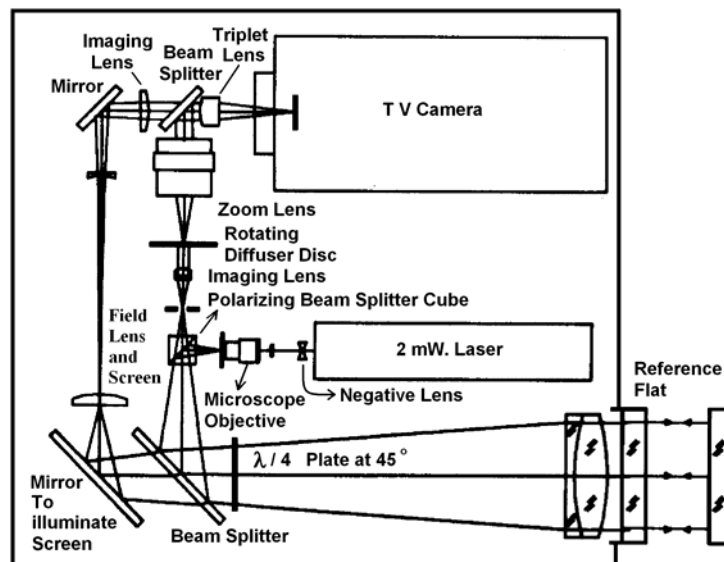


Fig. 4. The optical design of the laser interferometer Zygo GPI-XP.

## 2.2. Calibration of quartz rotation angles using linear polarized optical system

The experimental setup for calibration of quartz rotation plates consists of three main sections. The input quasi-monochromatic light section, the examining section and the output section. The input section contains a stabilized D. C. current source (SDC), a white light

source (LS) and a prism monochromator (M). The examining section consists of two items: a calcite Glan-Tomphson crystal polarizer (P) and an analyzer (A) that are mounted in rotating scales. The transmission axes of the crystals are set to be crossed and a stand for holding the examined quartz rotating plate is set between the crystals. The output section is composed of a sensing device which is a photomultiplier working by a stabilized high voltage power supply (max. 2000 volt) and the output D.C. current is measured by a digital multimeter as shown in Fig. 5. The experimental system is prepared, adjusted and the environmental conditions are adjusted applying a powerful air conditioning system. The system is switched on for enough time until all conditions are stable. Environmental temperature equals  $20^{\circ}\text{C} \pm 0.5^{\circ}\text{C}$  which is recorded and monitored using a digital thermometer of resolution  $0.1^{\circ}\text{C}$  since the quartz plate is sensitive to an increase in temperature [5].

The white light beams emitted from the source (LS) pass an aperture to eliminate the excess of intensity and strike the input narrow slit of the monochromator (M). Then, the light beams are transmitted from the output narrow slit. The quasi monochromatic light beams are normally incident on the polarizer (P) which converts them to a beam of linearly plane-polarized light propagating parallel to the polarizer transmission axis.

The initial situation is adjusted so that the polarizer and analyzer transmission axes are perpendicular to each other. In this case the linear plane waves parallel to the polarizer transmission axis will be stopped completely by the analyzer.

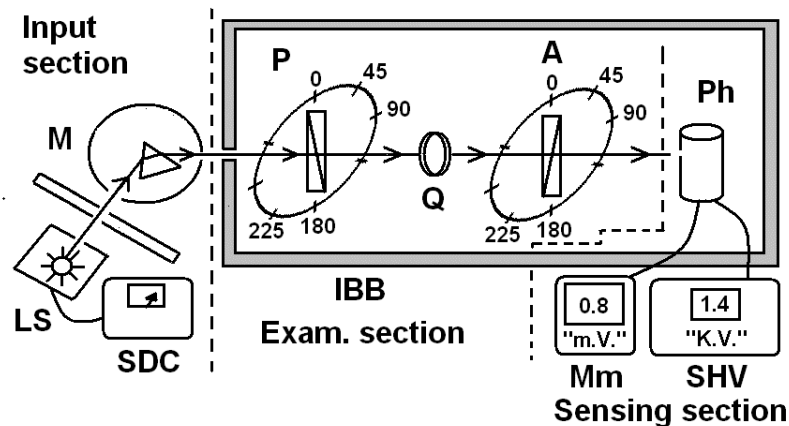


Fig. 5. The optical setup used for calibration of quartz plates rotation angles.

Then the quartz plate is inserted in the system and placed on a holder between the polarizer and the analyzer.

When the linear plane waves falls on the quartz plate it passes through it and rotates until it exits with rotation angle  $\beta$  given by Eq. (5). Therefore, the angle of emerging linear polarized beam will be equal to the angle of the polarizer transmission axis plus that of quartz rotation angle. Therefore the polarized beam angle will not be perpendicular to the analyzer axis transmission angle and can pass through the analyzer to the photomultiplier which converts the light intensity to a D. C. millivolt current measured by the multimeter.

To determine the quartz plate rotation angle, the analyzer is rotated slowly until the reading of the multimeter reaches a minimum. The angle of rotation of the analyzer is the angle of rotation of the quartz reference plate which is measured by a rotating scale with 360 degrees and a precision vernier with divisions of one minute ( $0.016^{\circ}$ ).

The setting of the perpendicularity of the polarizer and analyzer transmission axes is adjusted precisely to decrease the errors of the quartz rotation angles. The deviation of this setting is measured using the optical system shown in Fig. 5 without placing the quartz plate. This error is taken into consideration in the calibration of the quartz plate rotation angle.

### 3. RESULTS AND DISCUSSION

Quartz rotating angles plates are calibrated at a standard wavelength which equals 589.44 nm. Two quartz plates are calibrated, the first is type 34-20 and the second plate type 34-10. The nominal values of the quartz rotation plates in the manufacturer's certificate of calibration are  $34.66^\circ$  and  $33.66^\circ$  for the first and second quartz plates rotation angles respectively. The results of calibrations are plotted in a graph as shown in Fig. 6.

The results of calibrations for quartz plate type 34-20 are varying from  $34.49^\circ$  to  $34.76^\circ$  with a mean of  $34.645^\circ \pm 0.08223^\circ$ .

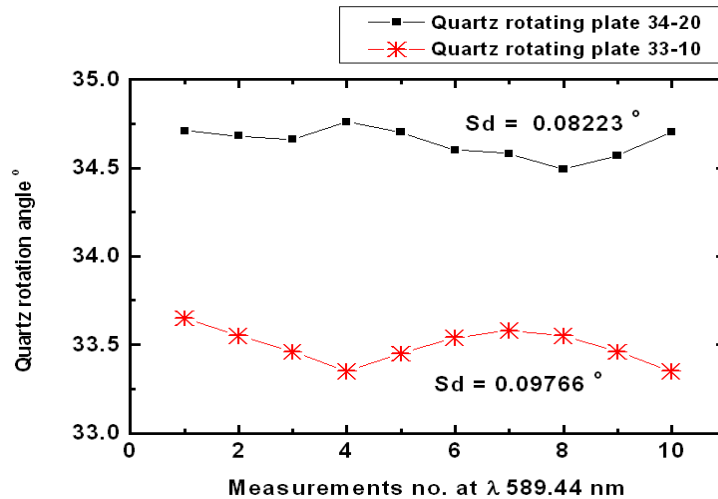


Fig. 6. Angles results of two quartz rotating plates (type 34-20, 34-10) are calibrated at  $\lambda$  (589.44 nm) with standard uncertainty  $Sd = \pm 0.082^\circ$  and  $\pm 0.097^\circ$ .

The results of the second plate type 34-10 are varying from  $33.35^\circ$  to  $33.65^\circ$  with a mean of  $33.494^\circ \pm 0.09766^\circ$ . The mean statistical uncertainty of calibration equals  $\pm 0.089945^\circ$  which is mathematically evaluated.

To study the effect of wavelength on reference standard quartz rotating plates the angles of rotation are measured several times using various wavelengths, applying the experimental optical setup discussed in section 2.2. The study includes the two quartz reference standard plates of different angles of rotation. The experimental results of the rotation angles can be accepted since the differences from nominal values are very small and are lying within the calibrations uncertainty limits. The differences of the angles of rotations of both quartz plates are caused by the differences in their thickness. The results of the relation dependence of the angle of rotation of quartz rotating plates on the applied monochromatic wavelength are plotted in Fig. 7.

The results shows that the relation between the quartz rotation angle and wavelength is an inverse relation since the quartz rotation angles are large at small wavelengths and decrease with increasing wavelength. The measurements of quartz rotation angles start from 420 nm to 680 nm in steps of 30 nm since the variation of angles are small.

The angles of rotation of the first quartz plate represented on Fig. 7 by solid circle are varying from 72 degree at 420 nm to 26.9 degrees at 680 nm. In case of the second plate rotation angles (denoted by stars, Fig. 7.) are varying from 69.15 degrees at 420 nm to 25.6 degrees at 680 nm. The difference between both quartz rotation angles are varying from -0.7 to 2.85 degrees. Since quartz rotation angles are calibrated at specific discrete wavelengths, a mathematical method is applied to evaluate the rotation angles across the entire calibration spectrum (400-700nm). The method fits curves to the calibrated quartz rotation angles results

using a second order polynomial regression to describe and determine the dependence of quartz angles on the wavelength. The applied mathematical method uses the following second order model:

$$Y = A + B_1X + B_2 X^2. \quad (6)$$

The fitted polynomial curves are denoted in Fig. 7 as solid and dashed lines representing the angles of rotations of the two quartz rotating plates types respectively.

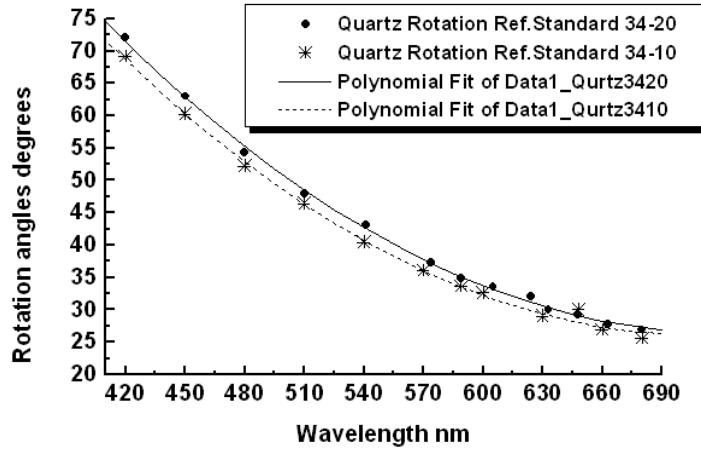


Fig. 7. The spectral dependence of the angles of the two quartz rotating plates applying monochromatic wavelengths.

The values of the angles of the first rotating quartz plate (34-20) are extrapolated with the model (6) and the equation of fitting is as follows:

$$Y = 285.09965^\circ - 0.71795 X^\circ + 4.98241 \times 10^{-4} X^{2^\circ}.$$

In case of the second quartz plate (34-10) the values of the angles are extrapolated with the model (6) and the equation of fitting is as follows:

$$Y = 280.57189^\circ - 0.71619 X^\circ + 5.03871 \times 10^{-4} X^{2^\circ}.$$

The R-Square values denoting the goodness of the fit for the calibrations of the 1<sup>st</sup> and 2<sup>nd</sup> quartz plates are 0.99871° with uncertainty of fitting (standard deviation of the fit to the model) ±0.57° and 0.9972° with uncertainty of fitting ±0.82° respectively with confidence interval equal to 95%.

The experimental values of quartz rotation angles can be applied to the determination of the rotation specific power ( $P_\lambda = \beta/d$  [6]) for both of the quartz plates. This can be realized applying the value of bi-rotation indices ( $n_L - n_R$ ) which equals  $7.1 \times 10^{-5}$ , calibrated at  $\lambda = 589.44$  nm [1] and Eq. (5) to determine the thickness of the quartz plates. The thickness of the first quartz plate 34-20 and the second plate 34-10 can be determined as follows:

$$d = \lambda \beta / 2\pi (n_L - n_R) \quad (7) \quad [1]$$

$$d(Q. p_{34-20}) = 1.605 \text{ mm and } d(Q. p_{34-10}) = 1.550 \text{ mm}$$

The rotation specific power ( $P_\lambda = \beta/d$ ) for both of the quartz plates can be given as follows:

$$P_{\lambda}(\text{Q. p 34-20}) = 21.682^{\circ} / \text{mm}, P_{\lambda}(\text{Q. p 34-10}) = 21.684^{\circ} / \text{mm}$$

The results of rotary specific powers of the Q plates verify the validity of the technique that is used to calibrate quartz rotating plates, since the difference between ( $P_{\lambda}$ ) for both plates equals 0.002 degrees/mm (7.2 Sec/mm).

Moreover the bi-rotation index values ( $n_L - n_R$ ) for all scanned wavelengths may be determined applying the experimental Q plate rotations and Eq. (5), as follows:

$$(n_L - n_R) = \beta \lambda / 2\pi d \quad (8)$$

The bi-rotation indices ( $n_L - n_R$ ) of quartz are plotted in a graph (Fig. 8).

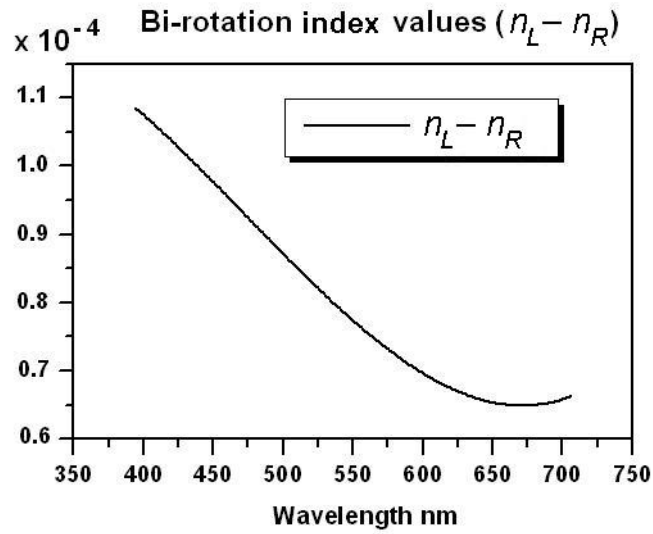


Fig. 8. Bi-rotation quartz index ( $n_L - n_R$ ) for all scanned wavelengths.

The quartz rotating plate (type 34-10) parallelism and surface roughness are examined as described in section 2.1, to study the effect of these metrological quantities on the rotation angles. These quantities are calibrated using the phase shifting laser interferometer. The results of surface roughness and parallelism of the quartz rotating plate surfaces are shown in Figs. 9 (a) and (b).

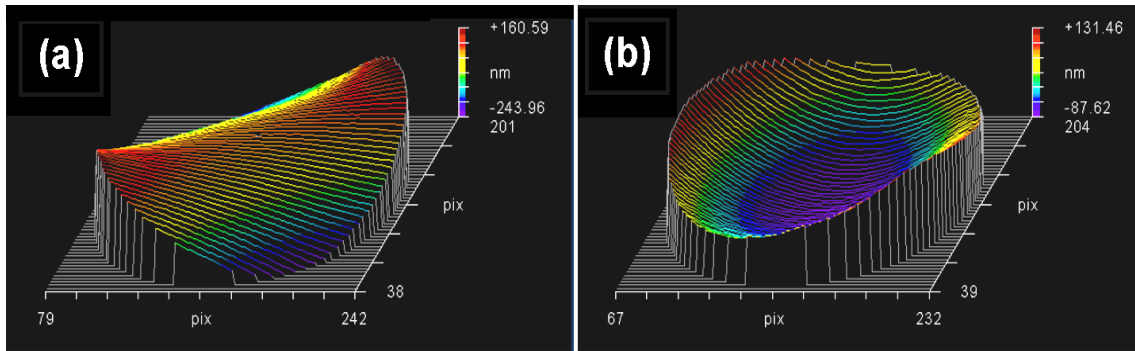


Fig. 9. Surface topography of quartz plates, a) 1<sup>st</sup> surface, P-V = 405 nm, with rms value = 84 nm, b) 2<sup>nd</sup> surface, P-V = 219 nm, with rms value = 53 nm.

Figures 9 (a) and (b) show the measurements of surface topography of both surfaces of the quartz rotating plate and results in a peak to valley value P-V = 405 nm, with roughness root mean square rms = 84 nm. (1<sup>st</sup> surface) and P-V = 219 nm, rms = 53 nm (2<sup>nd</sup> surface). The error of parallelism (0.65 sec) is determined as the angle between the two surfaces of the quartz plate measured by the Zygo interferometer setup shown in Fig. 3. The error of parallelism introduces an error to the thickness of quartz plate which equals:

$$e_t = L \tan 0.65 \text{ sec} = 0.0473 \text{ } \mu\text{m}. \quad (9)$$

Although this value is small, it can introduce an error to the measurements of rotation angles measured by  $\lambda = 589.44 \text{ nm}$ , which can be computed applying Eq. (5), as follows:

$$B(e_t) = 2\pi e_t (n_L - n_R) / \lambda = 0.001255395^\circ = (0^\circ 0' 3.69'').$$

The surface roughness of both plate surfaces cause a peak to valley error. Since both surfaces of the quartz rotating plates are opposite to each other, the P-V error for both surfaces will be equal to the difference between them, therefore,

$$\text{Total p-v} = 405 - 219 = 186 \text{ nm}.$$

This length can produce an error to the measurement of rotation angles at  $\lambda = 589.44 \text{ nm}$ , as follows:

$$B(e_{p-v}) = 2\pi e_{p-v} (n_L - n_R) / \lambda = 0.004033^\circ = (\pm 0^\circ 0' 14.52'').$$

The errors determined by interferometrical study that equals  $\pm 0.0050583^\circ = (\pm 0^\circ 0' 18.21'')$  is used for the evaluation of the uncertainty of the quartz rotation plate.

#### 4. QUARTZ ROTATING PLATES CALIBRATION UNCERTAINTY

The uncertainty of calibration of quartz rotation angles is evaluated using random and systematic uncertainties. The random uncertainty is evaluated by determining the standard deviation of the quartz rotation angles that are calibrated experimentally several times to allow for statistical evaluation of the uncertainty according to the method of the international Organization for Standardization, ISO [7].

The systematic uncertainty is determined using the results of measurements of surface roughness and the error of parallelism that affect the thickness of quartz plate and consequently affect quartz rotation angles.

The statistical uncertainty is calculated using the standard deviation of the mean of results [8] as follows:

$$u_j = \sqrt{\frac{1}{(n-1)} \sum_{j=1}^n (x_j - \bar{x})^2}, \quad (10)$$

where: n is the no. of measurements,  $x_j$  is the measured value,  $\bar{x}$  is the mean value.

Quartz rotation angles ( $\beta$ ) are calibrated with uncertainty  $(\Delta\beta) = \pm 0.089945^\circ$ .

Parallelism effect on quartz angles  $(\Delta\beta_p) = 0.001255395^\circ = (3'' .69)$ .

Surface roughness P-V effect on Q. angles  $(\Delta\beta_{p-v}) = \pm 0.004033^\circ = (0^\circ . 0' .14'' .52)$ .

The combined uncertainty of quartz rotation angles  $(\Delta\beta_t)$  includes all individual uncertainties [7, 8], can be determined as follows:

$$u\Delta\beta_t^2 = \left( u\Delta\beta^2 + u\Delta\beta_P^2 + u\Delta\beta_{P-V}^2 \right), \quad (11)$$

$$\begin{aligned} u\Delta\beta_t^2 &= \sqrt{[(\pm 0.089945^\circ)^2 + (0.001255395^\circ)^2 + (0.004033^\circ)^2]} = \\ &= \pm 0.0900441^\circ = \pm 0^\circ 5' 24''.16 \end{aligned}$$

The combined uncertainty of quartz rotation angles ( $\Delta\beta_t$ ) =  $\pm 0.0900441^\circ = \pm 0^\circ 5' 24''.16$

## 5. CONCLUSIONS

- 1- The relation dependence between the quartz plates rotation angles and the applied wavelength is calibrated using a linear polarized optical technique.
- 2- Quartz rotation angles of the  $\lambda$  range (420-680 nm) are determined applying extrapolation of the calibrated angles by polynomial regression fitting.
- 3- Rotation specific powers of quartz are determined and the validity of technique is verified since the difference between ( $P_\lambda$ ) for both plates equals 7.2 sec/mm.
- 4- The bi-rotation index values ( $n_L - n_R$ ) of the quartz rotation angles for all scanned wavelengths are determined applying the calibrated rotation angles.
- 5- The quartz rotating plate parallelism and surface roughness are studied and the effect of these metrological quantities on the Q rotation angles are calibrated and applied in the uncertainty evaluation of Q. Ref. plates. The combined uncertainty is evaluated for both calibrating techniques ( $\Delta\beta_t$ ) =  $\pm 0.09^\circ$ .

## ACKNOWLEDGEMENTS

We wish to thank the Arabian company for medicaments & medical plants and El-Farouk Company for Food Industries for allowing their quartz rotation plates to be studied in this article. Also, we thank dr. N. N. Nagib for providing some experimental facilities used in this work.

## REFERENCES

1. Hecht E., Zajac A.: *Optics*. Addison-Wesley Pub. Comp. 2<sup>nd</sup> edition 1977.
2. Wolf E.: *Progress in Optics*. N. Holland Pub. Comp. Amsterdam, vol. II, 1963.
3. Ditchburn R. W., F.R.S.: *Light*. Blackie & Son Ltd. London, 2<sup>nd</sup> edition 1963.
4. Operation manual: *Zygo GPI-Xp laser interferometer*, Zygo Cop. (USA).
5. Spec. manual: *Quartz Reference Plates*. Bellingham & Stanly Ltd. England.
6. Vyšín V., Vyšín I.: *Optical Rotatory Dispersion of  $\alpha$ -Quartz*. acta univ. palacki. olomuc., fac. rer. nat. (1997), physica 36, pp. 1-13.
7. *Guide To the Expression of Uncertainty in measurement*, 1995 International Organization for Standardization, ISO. 1995.
8. Hastings N.A.J., Peacock J.B.: *Statistical distributions*. London; Butterworth and Co., 1975.